Digital Signal Processing 96 (2020) 102600

Contents lists available at ScienceDirect

Digital Signal Processing

www.elsevier.com/locate/dsp

Low-complexity TDOA and FDOA localization: A compromise between two-step and DPD methods

Fuhe Ma [a,*], Fucheng Guo [a], Le Yang [b]

[a] State Key Laboratory of Complex Electromagnetic Environment Effects on Electronics and Information System, National University of Defense Technology, Changsha 410073, PR China

[b] Department of Electrical and Computer Engineering, University of Canterbury, Christchurch, 8020, New Zealand

ARTICLE INFO

Article history:
Available online 18 October 2019

Keywords:
Passive localization
Time difference of arrival (TDOA)
Frequency difference of arrival (FDOA)
Direct position determination (DPD)
Expectation maximization (EM)

ABSTRACT

Conventional two-step passive localization methods have poor localization precision when the input signal-to-noise ratio (SNR) is low, although they are usually computationally attractive. The direct position determination (DPD) methods, on the contrary, exhibit stronger robustness to low SNRs at the cost of much higher computational complexity. In this paper, an expectation-maximization (EM)-based computationally inexpensive localization method is proposed, which serves as a compromise between the two-step methods and DPD methods. During each iteration of the proposed method, the constraint that all intermediate parameters correspond to a common source position is taken into account explicitly, and this constraint is used to refine the time difference of arrival (TDOA) and frequency difference of arrival (FDOA) measurements. Then the source position is updated using these renewed measurements. The proposed method has superior localization performance under low SNR conditions compared to the two-step methods at the cost of limited increment in computational load, and its computational complexity is much lower than DPD methods at the cost of acceptable accuracy degradation. Moreover, the proposed method is applicable to other localization scenarios as well with appropriate modifications. Simulation results demonstrate the effectiveness of the proposed method.

1. Introduction

The problem of passive localization has received considerable research interest during the past decades. It is widely applied in fields such as emergency rescue, surveillance, and wireless sensor networks [1].

Conventional localization methods mostly fall into the two-step localization category [2–11]. In the first step, the location-dependent intermediate parameters are measured, such as the received signal strength (RSS), direction of arrival (DOA), time of arrival (TOA), time difference of arrival (TDOA) and frequency difference of arrival (FDOA). These intermediate parameters are further utilized to solve for the source position in the second step. Particularly, the localization system based on TDOA and FDOA does not require that the source signal transmission time be known, and only a single receiving channel is used at each observer. If the signal-to-noise ratio (SNR) is relatively high, the TDOA and FDOA are measured accurately, which would yield satisfactory localization performance [5,6,8–11]. In passive localization scenarios, however, the source to be localized are usually uncooperative, which may lead to low received SNR, especially when the source signal sidelobe is intercepted or when receiving antenna gain is not high enough. Under these circumstances, the localization accuracy of the two-step methods is relatively poor.

Recently, the direct position determination (DPD) methods have drawn much attention for their robustness to low SNR scenarios [12–18]. In most of the DPD methods, all the intercepted signals are transmitted to a central processing station to solve for the source position directly. As the cost function is constructed by relating directly received signals to source position, the constraint that all intermediate parameters correspond to a common source position is inherently applied during the DPD procedure [15]. In this way, the information loss caused by estimating intermediate parameters is avoided. Although empirical results validated that DPD methods performed much better than their two-step counterparts under low SNRs, the cost function of DPD methods is highly non-convex with a large number of local optimums, which entails an exhaustive grid search to find the global optimal solution [14,15,19]. This computationally demanding procedure hampers practical applications of DPD methods.

By noting the advantages and disadvantages of the two-step and DPD methods, one hopes to find a compromise between them,

* Corresponding author.
E-mail address: mafuhe14@nudt.edu.cn (F. Ma).

https://doi.org/10.1016/j.dsp.2019.102600
1051-2004/

which yields superior localization performance compared to two-step methods under low SNRs while being computationally efficient compared to the DPD methods. Unfortunately, there have been few works on this issue. In [20], three distributed DPD calculation methods were proposed to relieve the computational burden at the central processing node. The proposed methods made the system more robust to the loss of central processing node. In [21], the performances of two-step methods and DPD methods were analyzed for a multi-array DOA source positioning system. A new localization strategy was also proposed which combines the measurements obtained in the first step. However, the proposed method still belongs to the two-step localization category because all the angular parameters are measured independently. In [17], the authors proposed a novel expectation-maximization (EM)-based DPD method to solve the source position using time delay information for cooperative signals. The computational efficiency and the global convergence rate of the proposed method are relatively high. But it is tailored for cooperative TOA localization scenario only and not applicable to other localization schemes, such as time delay and Doppler information based source localization considered in this work.

In this paper, we propose an EM-based computationally inexpensive localization method using the time delay and Doppler information of received signals at multiple observers. By exploring the constraint inherently applied in DPD methods into the TDOA and FDOA estimation procedure during each iteration, the localization performance of the proposed method is improved compared to the two-step methods. Moreover, the source position is updated in closed form during each iteration instead of grid search, which makes the proposed method computationally much more efficient compared to the grid search DPD methods. As the development of the proposed method is in the form of an EM algorithm, it is guaranteed to converge, although local convergence may occur at a small probability. It should be mentioned that the proposed method is also applicable to other localization systems such as those based on AOA, TOA, etc., after appropriate modifications.

For brevity, the following notational conventions are used throughout this paper. $\|\cdot\|$ is the Euclidean norm of a given vector or ℓ_2-norm of a given matrix. $(\cdot)^T$, $(\cdot)^H$ and $(\cdot)^{-1}$ denote the transposition, the conjugate transposition and inverse operators, respectively. $\hat{(\cdot)}$ and $(\cdot)^0$ indicate the estimated value and true value of a variable. Further let $diag(\cdot)$ denote the diagonal matrix with main-diagonal elements taken from the given vector, $blkdiag\{\boldsymbol{A}_1, \boldsymbol{A}_2, \cdots, \boldsymbol{A}_M\}$ the block-diagonal matrix formed by $\boldsymbol{A}_1, \boldsymbol{A}_2, \cdots, \boldsymbol{A}_M$, $E_p\{\cdot\}$ the expectation over the distribution p, and $\lceil\cdot\rceil$ the ceiling operator. $\boldsymbol{O}$ and $\boldsymbol{I}$ represent the zero matrix and identity matrix, respectively, with their sizes derivable according to the context.

2. Problem formulation

For ease of illustration, a two-dimensional (2-D) localization scenario is considered in this paper, which can be extended to three-dimensional (3-D) scenario easily. The static source located at unknown position $\boldsymbol{u}^0 = [x_0, y_0]^T$ transmits radio signals, which are received by K spatially separated observers, with the position and velocity of observer k given by $\boldsymbol{p}_k = [x_k, y_k]^T$ and $\boldsymbol{v}_k = [\dot{x}_k, \dot{y}_k]^T$. It is assumed that the locations and velocities of observers are accurate, and the observer clocks are synchronized. When observer position/velocity errors and clock biases are present, the methods in [22,23] can be applied to calibrate the system.

The radio signal emitted from the source at time instant t is expressed as

$$s(t) = x(t)\exp\{j2\pi f_0 t\}, \tag{1}$$

where j is the unit imaginary number with $j^2 = -1$. $x(t)$ represents the baseband envelope of $s(t)$, and f_0 denotes the signal carrier frequency. Assume that the multi-path effect can be ignored, such that all received signals arrive at the observers through line-of-sight propagation. Thus the noise-free received signals at observers k can be written as

$$r_k^c(t) = \beta_k x\big((1+\alpha_k^0)t - \tau_k^0\big)\exp\big\{j2\pi f_0(1+\alpha_k^0)t\big\}, \tag{2}$$

where $\beta_k = a_k e^{-j2\pi f_0 \tau_k^0}$ with a_k denoting the unknown signal attenuation factor. τ_k^0 represents the signal propagation time from the source to the observer k, and α_k^0 indicates the Doppler scaling due to the relative motion. They are given by

$$\tau_k^0 = \frac{\|\boldsymbol{u}^0 - \boldsymbol{p}_k\|}{c}, \quad \alpha_k^0 = \frac{\boldsymbol{v}_k^T(\boldsymbol{u}^0 - \boldsymbol{p}_k)}{c\|\boldsymbol{u}_0 - \boldsymbol{p}_k\|}, \tag{3}$$

where we denoted by c the propagation speed of source signal. When the signal $s(t)$ is narrowband, i.e., the bandwidth B satisfies $B \ll f_0$, the narrowband approximation can be applied such that the Doppler scaling is approximated with a frequency shift. After frequency down conversion, the received noise-contaminated signal at observer k is given as

$$r_k(t) = a_k e^{j\phi_k} x(t - \tau_k^0)\exp\{j2\pi f_k^0 t\} + w_k(t), \tag{4}$$

where $f_k^0 = f_0\alpha_k^0$ is the Doppler frequency shift, and ϕ_k is the phase shift which takes into account the term $-2\pi f_0\tau_k^0$ and the unknown phase of local oscillator. $w_k(t)$ denotes the additive white Gaussian noise with zero mean and known variance σ_n^2, and it is usually assumed that the noises are uncorrelated across different observers over different time instants. As the source signal is uncooperative, $x(t)$ and its distribution are not available. A common practice is to take the unknown noise-free received signal at observer 1 (reference observer) as the reference signal, so that $r_k(t), k = 2, 3, \cdots, K$ in (4) could be reformulated as

$$r_k(t) = a_{k,1}e^{j\phi_{k,1}} r_1^0(t - \tau_{k,1}^0)e^{j2\pi f_{k,1}^0 t} + w_k(t) \tag{5}$$

where

$$\begin{aligned} \tau_{k,1}^0 &= \tau_k^0 - \tau_1^0 \\ f_{k,1}^0 &= f_k^0 - f_1^0, \end{aligned} \tag{6}$$

and $r_1^0(t)$ is the unknown noiseless version of $r_1(t)$. $a_{k,1} = a_k/a_1$ is real-valued relative gain between the signals received at observer k and observer 1. $\phi_{k,1} = \phi_k - \phi_1$ represents the unknown phase offset.

Sampling $r_k(t)$ discretely at a uniform interval $t_s = 1/f_s$ with f_s being the sampling frequency such that $r_k(n) \equiv r_k(t = nt_s)$, the notation for transmission time, i.e., t is removed and the received discrete signal of length N is given by [24]

$$\boldsymbol{r}_k = b_{k,1}\boldsymbol{D}_{f,k}(f_{k,1}^0)\boldsymbol{D}_{\tau,k}(\tau_{k,1}^0)\boldsymbol{r}_1^0 + \boldsymbol{w}_k, \tag{7}$$

where $\boldsymbol{r}_k = [r_k(1), \cdots, r_k(N)]^T$. $\boldsymbol{r}_1^0 = [r_1^0(1), \cdots, r_1^0(N)]^T$ denotes the noiseless reference signal vector at the reference observer. $b_{k,1} = a_{k,1}e^{j\phi_{k,1}}$ is the complex relative gain, and $\boldsymbol{w}_k = [w_k(1), \cdots, w_k(N)]^T$. For given TDOA $\tau_{k,1}$ and FDOA $f_{k,1}$, we have

$$\begin{aligned} \boldsymbol{D}_{f,k}(f_{k,1}) &= diag\left\{\exp\{j2\pi f_{k,1}(N/2 + \boldsymbol{n})\}\right\} \\ \boldsymbol{D}_{\tau,k}(\tau_{k,1}) &= \boldsymbol{F}^H diag\left\{\boldsymbol{\Gamma}_{k,1}(\tau_{k,1})\right\}\boldsymbol{F}, \end{aligned} \tag{8}$$

which signify the Doppler frequency shift and time delay operators, respectively, where $\boldsymbol{\Gamma}_{k,1}(\tau_{k,1}) = \exp\{-j2\pi\frac{f_s}{N}\boldsymbol{n}\tau_{k,1}\}$ and $\boldsymbol{n} = [-N/2, -N/2+1, \cdots, N/2-1]^T$. $\boldsymbol{F} = \frac{1}{\sqrt{N}}\exp\{-j2\pi\boldsymbol{n}\boldsymbol{n}^T/N\}$ is

the fast Fourier transform (FFT) matrix. Define $\boldsymbol{Q}_{k,1}(\tau_{k,1}^0, f_{k,1}^0) = \boldsymbol{D}_{f,k}(f_{k,1}^0)\boldsymbol{D}_{\tau,k}(\tau_{k,1}^0)$, such that (7) can be reformulated compactly as

$$\boldsymbol{r}_k = b_{k,1}\,\boldsymbol{Q}_{k,1}(\tau_{k,1}^0, f_{k,1}^0)\boldsymbol{r}_1^0 + \boldsymbol{w}_k. \tag{9}$$

When all observers are stationary, there is no Doppler effect caused by relative motion between the source and observers, i.e., $f_{k,1}^0 = 0$. Under this condition, one can obtain $\boldsymbol{D}_{f,k} = \boldsymbol{I}$, and the signal model degenerates into a TDOA positioning one.

Our aim is to determine the source position $\boldsymbol{u}^0$ using all the received signals $\boldsymbol{r} = [\boldsymbol{r}_1^T, \boldsymbol{r}_2^T, \cdots, \boldsymbol{r}_K^T]^T$. In next section, the cost functions of two-step and DPD methods are retrieved to highlight the differences between them and to make our proposed method more accessible.

3. Comparison of two-step and DPD methods

In this section, we compare and analyze the differences between the two-step and DPD methods regarding their cost functions and source positioning procedures. First define $\boldsymbol{u}$ as an arbitrarily given source position. As the measurement noise $\boldsymbol{w}_k$ is independently Gaussian distributed for $k = 1, 2, \cdots, K$, the log likelihood function of signal vector $\boldsymbol{r}$ with respect to the source position $\boldsymbol{u}$, the unknown $\boldsymbol{r}_1^0$ and the relative gain $\boldsymbol{b}$ is given by

$$\begin{aligned}&\ln P(\boldsymbol{r}|\boldsymbol{u}, \boldsymbol{r}_1^0, \boldsymbol{b})\\ &= c_0 - \frac{1}{2\sigma_n^2}\sum_{k=1}^{K}\left\|\boldsymbol{r}_k - b_{k,1}\,\boldsymbol{Q}_{k,1}(\tau_{k,1}(\boldsymbol{u}), f_{k,1}(\boldsymbol{u}))\boldsymbol{r}_1^0\right\|^2,\end{aligned} \tag{10}$$

where c_0 is a constant independent of $\boldsymbol{u}$, $\boldsymbol{b} = [b_{2,1}, \cdots, b_{K,1}]^T$. Obviously we have $b_{1,1} = 1$, $\boldsymbol{Q}_{1,1}\big(\tau_{1,1}(\boldsymbol{u}), f_{1,1}(\boldsymbol{u})\big) = \boldsymbol{I}$ according to their definitions. $\tau_{k,1}(\boldsymbol{u})$ and $f_{k,1}(\boldsymbol{u})$ are obtained by substituting $\boldsymbol{u}$ into (6).

As the noise variance σ_n^2 is independent of source position, scaling the log likelihood function above and ignoring irrelevant terms, the generic cost function is given by

$$\begin{aligned}C(\boldsymbol{u}, \boldsymbol{r}_1^0, \boldsymbol{b}) &= \sum_{k=1}^{K} C(\boldsymbol{u}, \boldsymbol{r}_1^0, \boldsymbol{b}, k)\\ &= \sum_{k=1}^{K}\left\|\boldsymbol{r}_k - b_{k,1}\,\boldsymbol{Q}_{k,1}(\tau_{k,1}(\boldsymbol{u}), f_{k,1}(\boldsymbol{u}))\boldsymbol{r}_1^0\right\|^2.\end{aligned} \tag{11}$$

3.1. DPD methods

For the DPD methods, the intermediate parameters $\tau_{k,1}^0$ and $f_{k,1}^0$ are not estimated and one seeks to estimate $\boldsymbol{u}^0$ from the received $\boldsymbol{r}$ directly. The unknown relative amplitudes $b_{k,1}, k = 2, 3, \cdots, K$ are considered as nuisance parameters and their maximum-likelihood (ML) estimates can be obtained by taking the partial derivative of (11) with respect to $b_{k,1}$ and setting it to zero, which yield [13,18]

$$\hat{b}_{k,1} = \frac{(\boldsymbol{r}_1^0)^H\,\boldsymbol{Q}_{k,1}^H\big(\tau_{k,1}(\boldsymbol{u}), f_{k,1}(\boldsymbol{u})\big)\boldsymbol{r}_k}{\|\boldsymbol{r}_1^0\|^2}. \tag{12}$$

Substituting $\hat{b}_{k,1}$ into (11), ignoring irrelevant terms and after some straightforward mathematical manipulations, one has the simplified cost function given by

$$C_1(\boldsymbol{u}, \boldsymbol{r}_1^0) = (\boldsymbol{r}_1^0)^H\boldsymbol{V}\boldsymbol{V}^H\boldsymbol{r}_1^0/\|\boldsymbol{r}_1^0\|^2, \tag{13}$$

where

$$\begin{aligned}\boldsymbol{V} = [&\boldsymbol{r}_1,\ \boldsymbol{Q}_{2,1}^H\big(\tau_{2,1}(\boldsymbol{u}), f_{2,1}(\boldsymbol{u})\big)\boldsymbol{r}_2, \cdots,\\ &\boldsymbol{Q}_{K,1}^H\big(\tau_{K,1}(\boldsymbol{u}), f_{K,1}(\boldsymbol{u})\big)\boldsymbol{r}_K].\end{aligned} \tag{14}$$

As $\boldsymbol{r}_1^0$ is also unknown, to maximize (13) we simply set $\boldsymbol{r}_1^0/\|\boldsymbol{r}_1^0\|$ as the eigenvector corresponding to the maximal eigenvalue of $\boldsymbol{V}\boldsymbol{V}^H$. Then the DPD cost function can be given as [13]

$$C_{direct}(\boldsymbol{u}) = \lambda_{max}(\boldsymbol{V}\boldsymbol{V}^H), \tag{15}$$

where $\lambda_{max}(\cdot)$ denotes the maximal eigenvalue of a given square matrix. However, with large signal length N the dimension of $\boldsymbol{V}\boldsymbol{V}^H$ could be very high and performing eigenvalue decomposition on $\boldsymbol{V}\boldsymbol{V}^H$ could be computationally very demanding. Note that the nonzero eigenvalues of $\boldsymbol{V}\boldsymbol{V}^H$ are equivalent to that of $\boldsymbol{V}^H\boldsymbol{V}$, one can alternatively define $C_{direct}(\boldsymbol{u})$ as the maximal eigenvalue of the K-dimensional $\boldsymbol{V}^H\boldsymbol{V}$. The source position estimate is thus given by

$$\begin{aligned}\hat{\boldsymbol{u}} &= \arg\max_{\boldsymbol{u}} C_{direct}(\boldsymbol{u})\\ &= \lambda_{max}(\boldsymbol{V}^H\boldsymbol{V}).\end{aligned} \tag{16}$$

The cost function $C_{direct}(\boldsymbol{u})$ is highly non-convex and multimodal with a considerable number of local maximums. The commonly applied method to find global optimum is grid search, which is known for its high computational complexity, especially when the source localization scenario is in 3-D and relatively high localization precision is required. However, as revealed in (14) and (16), the source position is estimated directly from the received signals without estimating TDOA and FDOA. In this way, the constraint that all $\tau_{k,1}$ and $f_{k,1}$ correspond to the same source position is inherently applied when one solves (16). Thus the DPD methods generally exhibit superior performance compared with the two-step methods under low SNR conditions. Next the cost function for the two-step localization is provided.

3.2. Conventional two-step methods

In the two-step methods, the constraint that all TDOAs and FDOAs are correlated according to the source position is relaxed such that (11) can be decomposed into $C(\boldsymbol{u}, \boldsymbol{r}_1^0, \boldsymbol{b}, k)$ for $k = 2, 3, \cdots, K$, each parameterized by $\tau_{k,1}$ and $f_{k,1}$ respectively. Thus TDOA/FDOA between observer $k, k = 2, 3, \cdots, K$ and reference observer could be estimated independently. Then these TDOAs/FDOAs are transferred to the central processing station to solve for the source position efficiently via semi-definite relaxation and closed-form solvers during the second step [5,6,8–11].

Classical TDOA and FDOA estimation methods mostly involve finding the peak of the cross-ambiguity function (CAF) via interpolating the CAF surface. The cost function for estimating the TDOA and FDOA between observer k and reference observer is given by [25,26]

$$C_{s1}(\tau, f, k) = |\boldsymbol{r}_1^H\,\boldsymbol{Q}_{k,1}^H(\tau, f)\boldsymbol{r}_k|, \tag{17}$$

and thus TDOA and FDOA estimates are given by

$$[\hat{\tau}_{k,1}, \hat{f}_{k,1}] = \arg\max_{\tau, f} C_{s1}(\tau, f, k). \tag{18}$$

Collecting and stacking the measured TDOAs and FDOAs in a vector $\boldsymbol{\theta} = [\hat{\tau}_{2,1}, \hat{f}_{2,1}, \cdots, \hat{\tau}_{K,1}, \hat{f}_{K,1}]^T$, and their covariance in a composite matrix $\boldsymbol{\Lambda} = E\{(\boldsymbol{\theta} - \boldsymbol{\theta}^0)(\boldsymbol{\theta} - \boldsymbol{\theta}^0)^T\}$ where $\boldsymbol{\theta}^0 = [\tau_{2,1}^0, f_{2,1}^0, \cdots, \tau_{K,1}^0, f_{K,1}^0]^T$. The ML cost function for the source position determination in the second step is given by [5]

$$C_{s2}(\boldsymbol{u}) = (\boldsymbol{\theta} - \boldsymbol{\theta}(\boldsymbol{u}))^T\boldsymbol{\Lambda}^{-1}(\boldsymbol{\theta} - \boldsymbol{\theta}(\boldsymbol{u})), \tag{19}$$

where $\boldsymbol{\theta}(\boldsymbol{u})$ denotes the predicted TDOA and FDOA vector obtained by substituting $\boldsymbol{u}$ into (6). The source position estimate is thereby obtained by

$$\hat{\boldsymbol{u}} = \arg\min_{\boldsymbol{u}} C_{s2}(\boldsymbol{u}). \tag{20}$$

As the covariance matrix $\boldsymbol{\Lambda}$ is usually not known *a priori*, the CRLB for TDOA and FDOA estimation is used instead [24]. The solution for the cost function in (19) can be obtained quite efficiently as mentioned before.

From (17) and (19), one can find that the two-step methods relax the constraint and introduce intermediate parameters to make the cost function in (11) decoupled for each observer pair. To be specific, the TDOA and FDOA between observer k and observer 1 are estimated independently, without considering the constraint that all $\tau_{k,1}^0$ and $f_{k,1}^0$ correspond to a common source position $\boldsymbol{u}^0$. The lines of positioning do not intersect at a single point. Therefore, the two-step methods are suboptimal in this sense compared to DPD methods and its localization accuracy degrades significantly under low SNRs. However, as the two steps in (18) and (20) can be solved successively with relatively low computational cost, the two-step methods are computationally very efficient compared to DPD methods.

In next section, we proceed to present a novel EM-based localization method, which serves as a compromise between the DPD methods and the two-step methods.

4. Proposed method

According to the discussions in Section 3, if we introduce the constraint that, all intermediate parameters are correlated according to the source position, into the two-step localization framework, we may improve the localization performance of two-step methods under low SNR conditions while making the computational cost lower compared with DPD methods. With this regards, an EM-based localization method is proposed in the following, of which the E step and M step correspond to the first and second steps of the two-step localization procedure, respectively. However, different from the two-step methods, the constraint that all TDOAs and FDOAs correspond to a common source position is taken into consideration to refine the TDOA and FDOA estimates during the E step, thus the source position could be refined in closed-form during the M step. In this way, the proposed method is computationally inexpensive compared to grid search DPD methods but with superior performance at low SNRs over the two-step approaches.

4.1. Proposed EM localization method

To embed the constraint on TDOAs and FDOAs into their estimation procedures so as to improve the localization performance, we propose to estimate the intermediate TDOA and FDOA parameters and the source position iteratively. On the one hand, the source position provides a constraint to the TDOAs and FDOAs when they are estimated. On the other hand, these updated TDOAs and FDOAs could refine the source position in return. To achieve this goal, the celebrated EM algorithm is resorted to, which is widely applied to decouple the high-dimensional parameter estimation problems into multiple low-dimensional ones [27]. In our proposed method, the observed $\boldsymbol{r}$ is defined as incomplete data, which is combined with the hidden data, i.e., the noisy TDOA and FDOA measurement vector $\boldsymbol{\theta}$, to form the complete data $\boldsymbol{z} = [\boldsymbol{r}^T, \boldsymbol{\theta}^T]^T$.

The log likelihood function of the complete data $\boldsymbol{z}$ is given by

$$\begin{aligned}\ln P(\boldsymbol{z}|\boldsymbol{u}) &= \ln P(\boldsymbol{r}|\boldsymbol{\theta}, \boldsymbol{u}) + \ln P(\boldsymbol{\theta}|\boldsymbol{u}) \\ &= \ln P(\boldsymbol{r}|\boldsymbol{\theta}) + \ln P(\boldsymbol{\theta}|\boldsymbol{u}),\end{aligned} \tag{21}$$

where we have used the fact that, $\boldsymbol{r}$ is conditionally independent of $\boldsymbol{u}$ given $\boldsymbol{\theta}$, in the second line of (21). $\ln P(\boldsymbol{r}|\boldsymbol{\theta})$ can be approximately given by [26]

$$\ln P(\boldsymbol{r}|\boldsymbol{\theta}) = \frac{1}{\sigma_n^2} \sum_{k=2}^{K} \frac{|\hat{b}_{k,1}|}{1+|\hat{b}_{k,1}|^2} \left| \boldsymbol{r}_k^H \boldsymbol{Q}_{k,1}(\boldsymbol{\theta}) \boldsymbol{r}_1 \right|, \tag{22}$$

where $\hat{b}_{k,1}$ is obtained by plugging $\tau_{k,1}$ and $f_{k,1}$ in $\boldsymbol{\theta}$ into (12) with $\boldsymbol{r}_1^0$ replaced by $\boldsymbol{r}_1$.

As $\boldsymbol{\theta}$ is noise contaminated due to the noisy $\boldsymbol{r}$, $\ln P(\boldsymbol{\theta}|\boldsymbol{u})$ is given by

$$\ln P(\boldsymbol{\theta}|\boldsymbol{u}) = -\frac{1}{2}\big(\boldsymbol{\theta} - \boldsymbol{\theta}(\boldsymbol{u})\big)^T \boldsymbol{\Lambda}^{-1} \big(\boldsymbol{\theta} - \boldsymbol{\theta}(\boldsymbol{u})\big), \tag{23}$$

where $\boldsymbol{\Lambda}$ is the covariance matrix of $\boldsymbol{\theta}$ as defined above.

E step: Assume that after the mth iteration one has already obtained the current source position estimate $\hat{\boldsymbol{u}}^{(m)}$ and the corresponding source position covariance matrix $\boldsymbol{\Sigma}^{(m)}$, where the superscript $(\cdot)^{(m)}$ denotes the index of iteration. For the E step of the EM algorithm, the TDOA/FDOA vector $\boldsymbol{\theta}$ is estimated by maximizing the conditional probability density function (pdf) of $\boldsymbol{\theta}$ given the current source position estimate $\hat{\boldsymbol{u}}^{(m)}$ as well as the observed $\boldsymbol{r}$, i.e., $\boldsymbol{\theta}^{(m+1)} = \arg\max_{\boldsymbol{\theta}} P(\boldsymbol{\theta}|\hat{\boldsymbol{u}}^{(m)}, \boldsymbol{r})$, where $\boldsymbol{\theta}^{(m+1)} = [(\boldsymbol{\theta}_{2,1}^{(m+1)})^T, \cdots, (\boldsymbol{\theta}_{K,1}^{(m+1)})^T]^T$, and where $P(\boldsymbol{\theta}|\hat{\boldsymbol{u}}^{(m)}, \boldsymbol{r})$ is given by

$$\begin{aligned}P(\boldsymbol{\theta}|\hat{\boldsymbol{u}}^{(m)}, \boldsymbol{r}) &= \frac{P(\boldsymbol{\theta}, \boldsymbol{r}|\hat{\boldsymbol{u}}^{(m)})}{P(\boldsymbol{r}|\hat{\boldsymbol{u}}^{(m)})} \propto P(\boldsymbol{\theta}|\hat{\boldsymbol{u}}^{(m)}) P(\boldsymbol{r}|\boldsymbol{\theta}) \\ &= c_1 \exp\left\{ \frac{1}{\sigma_n^2} \sum_{k=2}^{K} \frac{|\hat{b}_{k,1}|}{1+|\hat{b}_{k,1}|^2} \left| \boldsymbol{r}_k^H \boldsymbol{Q}_{k,1}(\boldsymbol{\theta}) \boldsymbol{r}_1 \right| \right\} \\ &\quad \times \exp\left\{ -\frac{1}{2} (\boldsymbol{\theta} - \boldsymbol{\theta}(\hat{\boldsymbol{u}}^{(m)}))^T (\boldsymbol{\Lambda}^{(m)})^{-1} (\boldsymbol{\theta} - \boldsymbol{\theta}(\hat{\boldsymbol{u}}^{(m)})) \right\},\end{aligned} \tag{24}$$

where c_1 is a constant independent of $\boldsymbol{\theta}$, and $\boldsymbol{\Lambda}^{(m)}$ is the covariance matrix of $\boldsymbol{\theta}$ after the mth iteration. Obviously (24) could be solved with respect to each $\boldsymbol{\theta}_{k,1}^{(m+1)}$ independently.

Note that distinctive from the first step of the two-step methods, the correlation of $\boldsymbol{\theta}$ with respect to $\boldsymbol{u}$ has been embedded in (24). The resultant TDOA and FDOA are expected to be more robust to low SNR conditions compared with conventional two-step methods. In the following we manage to obtain the TDOA and FDOA estimate $\boldsymbol{\theta}^{(m+1)}$ via maximizing (24).

The maximizers $\boldsymbol{\theta}_{k,1}^{(m+1)}, k = 2, 3, \cdots, K$ of (24) are usually obtained via grid search and cannot be solved in closed-form due to the high nonlinearity of $P(\boldsymbol{\theta}|\hat{\boldsymbol{u}}^{(m)}, \boldsymbol{r})$ with respect to $\boldsymbol{\theta}$. As an alternative, we propose to obtain an approximated solution via computationally efficient Gaussian weighted summation, i.e., the weighted summation of predicted TDOA/FDOA vector $\tilde{\boldsymbol{\theta}}_{k,1} = [\tilde{\tau}_{k,1}, \tilde{f}_{k,1}]^T$ and estimated TDOA/FDOA $\bar{\boldsymbol{\theta}}_{k,1} = [\bar{\tau}_{k,1}, \bar{f}_{k,1}]^T$ for $k = 2, 3, \cdots, K$, where $\tilde{\tau}_{k,1} = \tau_{k,1}(\hat{\boldsymbol{u}}^{(m)})$ and $\tilde{f}_{k,1} = f_{k,1}(\hat{\boldsymbol{u}}^{(m)})$ are TDOA and FDOA predictions evaluated at the current source position estimate $\hat{\boldsymbol{u}}^{(m)}$. The Gaussian weighted summation procedure is given in the following.

On the one hand, substituting the current source position estimate $\hat{\boldsymbol{u}}^{(m)}$ into (6) yields the TDOA and FDOA prediction vector $\tilde{\boldsymbol{\theta}}_{k,1}$ between observer k and reference observer. Although it is obvious that the predicted TDOA and FDOA vector does not follow a Gaussian distribution, one can approximate this non-Gaussian distribution with a Gaussian distribution as applied in non-linear filtering [28]. The corresponding covariance matrix of $\tilde{\boldsymbol{\theta}}_{k,1}$ is approximated as

$$\tilde{\boldsymbol{\Lambda}}_{k,1} = \boldsymbol{G}_{k,1}^T(\hat{\boldsymbol{u}}^{(m)})\boldsymbol{\Sigma}^{(m)}\boldsymbol{G}_{k,1}(\hat{\boldsymbol{u}}^{(m)}), \tag{25}$$

where $\boldsymbol{G}_{k,1}(\hat{\boldsymbol{u}}^{(m)}) = [\frac{\partial \tau_{k,1}}{\partial \boldsymbol{u}}, \frac{\partial f_{k,1}}{\partial \boldsymbol{u}}]\big|_{\boldsymbol{u}=\hat{\boldsymbol{u}}^{(m)}}$ is the Jacobian matrix composed of partial derivatives of $\tau_{k,1}$ and $f_{k,1}$ with respect to the source position evaluated at $\hat{\boldsymbol{u}}^{(m)}$.

On the other hand, for the evaluation of $\bar{\boldsymbol{\theta}}_{k,1}$, one can readily define the 3σ confidence region of the TDOA $\tau_{k,1}$ and FDOA $f_{k,1}$ determined by $\tilde{\boldsymbol{\theta}}_{k,1}$ and $\tilde{\boldsymbol{\Lambda}}_{k,1}$, i.e.,

$$\begin{aligned} \bar{\tau}_{k,1} &\in [\tilde{\tau}_{k,1} - 3\sigma_\tau, \tilde{\tau}_{k,1} + 3\sigma_\tau] \\ \bar{f}_{k,1} &\in [\tilde{f}_{k,1} - 3\sigma_f, \tilde{f}_{k,1} + 3\sigma_f], \end{aligned} \tag{26}$$

where σ_τ and σ_f are respectively, the square root of the main-diagonal entries of $\tilde{\Lambda}_{k,1}$, indicating the TDOA and FDOA standard deviation (SD). By finding the peak within this confidence region on the 2-D CAF surface and interpolating, the resultant TDOA and FDOA estimates ($\bar{\tau}_{k,1}$ and $\bar{f}_{k,1}$) are obtained. For the evaluation of their covariance $\bar{\boldsymbol{\Lambda}}_{k,1}$, it is a common practice to obtain it using the CRLB expression [24].

According to the property of Gaussian distribution, the updated TDOA and FDOA sub-vector $\boldsymbol{\theta}_{k,1}^{(m+1)}$ as well as its covariance matrix is obtained using weighted summation as [29]

$$\boldsymbol{\theta}_{k,1}^{(m+1)} = \boldsymbol{\Lambda}_{\tau,f,k,1}^{(m+1)}(\bar{\boldsymbol{\Lambda}}_{k,1}^{-1}\bar{\boldsymbol{\theta}}_{k,1} + \tilde{\boldsymbol{\Lambda}}_{k,1}^{-1}\tilde{\boldsymbol{\theta}}_{k,1}), \tag{27}$$

and

$$\boldsymbol{\Lambda}_{\tau,f,k,1}^{(m+1)} = (\bar{\boldsymbol{\Lambda}}_{k,1}^{-1} + \tilde{\boldsymbol{\Lambda}}_{k,1}^{-1})^{-1}. \tag{28}$$

In this way, one could obtain the updated TDOA and FDOA vector $\boldsymbol{\theta}^{(m+1)}$ and the corresponding covariance matrix $\boldsymbol{\Lambda}^{(m+1)} = \text{blkdiag}\{\boldsymbol{\Lambda}_{\tau,f,2,1}^{(m+1)}, \boldsymbol{\Lambda}_{\tau,f,3,1}^{(m+1)} \cdots, \boldsymbol{\Lambda}_{\tau,f,K,1}^{(m+1)}\}$.

M step: The auxiliary function to be maximized in EM algorithm is given by [27]

$$T(\boldsymbol{u}|\hat{\boldsymbol{u}}^{(m)}) = \mathrm{E}_{P(\boldsymbol{\theta}|\hat{\boldsymbol{u}}^{(m)},\boldsymbol{r})}\{\ln P(\boldsymbol{z}|\boldsymbol{u})\}. \tag{29}$$

Using the Laplacian approximation [30] and noticing that the term $\ln P(\boldsymbol{r}|\boldsymbol{\theta})$ in $\ln P(\boldsymbol{z}|\boldsymbol{u})$ is conditionally independent of $\boldsymbol{u}$, one can approximate the auxiliary function as

$$\begin{aligned} &T(\boldsymbol{u}|\hat{\boldsymbol{u}}^{(m)}) \approx \ln P(\boldsymbol{\theta}^*|\boldsymbol{u}) \\ &\quad s.t. \quad \boldsymbol{\theta}^* = \arg\max_{\boldsymbol{\theta}} P(\boldsymbol{\theta}|\hat{\boldsymbol{u}}^{(m)}, \boldsymbol{r}). \end{aligned} \tag{30}$$

Since we have just obtained the maximizer $\boldsymbol{\theta}^* = \boldsymbol{\theta}^{(m+1)}$ during the E step, the source position is updated in the M step by maximizing the auxiliary function

$$\begin{aligned} \hat{\boldsymbol{u}}^{(m+1)} &= \arg\max_{\boldsymbol{u}} T(\boldsymbol{u}|\hat{\boldsymbol{u}}^{(m)}) \\ &= \arg\max_{\boldsymbol{u}} \ln P(\boldsymbol{\theta}^{(m+1)}|\boldsymbol{u}). \end{aligned} \tag{31}$$

Note that solving (31) is equivalent to the second step of the conventional two-step methods, and thus the updated source position $\hat{\boldsymbol{u}}^{(m+1)}$ could be obtained efficiently using the closed-form solvers [5,6,9,31] instead of grid search as applied in DPD methods. The updated covariance matrix of source position is approximately given by

$$\boldsymbol{\Sigma}^{(m+1)} = \left(\boldsymbol{G}(\hat{\boldsymbol{u}}^{(m+1)})(\boldsymbol{\Lambda}^{(m+1)})^{-1}\boldsymbol{G}^T(\hat{\boldsymbol{u}}^{(m+1)})\right)^{-1}, \tag{32}$$

where

$$\boldsymbol{G}(\hat{\boldsymbol{u}}^{(m+1)}) = \left[\boldsymbol{G}_{2,1}(\hat{\boldsymbol{u}}^{(m+1)}), \cdots, \boldsymbol{G}_{K,1}(\hat{\boldsymbol{u}}^{(m+1)})\right]. \tag{33}$$

Repeating the E-step and M-step elaborated above, the source position update sequence is expected to converge to the proximity of $\boldsymbol{u}^0$, and the proposed method stops when $\|\hat{\boldsymbol{u}}^{(m+1)} - \hat{\boldsymbol{u}}^{(m)}\|$ is within a given tolerance.

4.2. Details of the proposed method

In this part, details about the proposed method are given.

4.2.1. Implementation of the propose method

For the setup of source position initial value, i.e., $\hat{\boldsymbol{u}}^{(0)}$, one can choose it randomly within the region of interest when this region is not so large. For a relatively large region, multiple initial points may be needed for the proposed method to reduce the probability of converging to local optimal solutions. To achieve this, one can divide the *a priori* region uniformly into N_p blocks with D_x and D_y being respectively, the block widths along X and Y directions, and the center of each block is selected as an initial source position, with the initial covariance matrix given by $\boldsymbol{\Sigma}^{(0)} = diag([\frac{D_x^2}{12}, \frac{D_y^2}{12}])$. For each initial position $\hat{\boldsymbol{u}}_p^{(0)}, p = 1, 2, \cdots, N_p$, use the proposed EM-based iterative method to obtain the estimate $\hat{\boldsymbol{u}}_p$, and the final source position estimate is given by choosing among all the estimates $\hat{\boldsymbol{u}}_p, p = 1, 2, \cdots, N_p$ the one with the maximal CAF surface summations

$$\hat{\boldsymbol{u}} = \arg\max_{\hat{\boldsymbol{u}}_p} \sum_{k=2}^{K} |\boldsymbol{r}_1^H \boldsymbol{Q}_{k,1}^H(\tau(\hat{\boldsymbol{u}}_p), f(\hat{\boldsymbol{u}}_p))\boldsymbol{r}_k|. \tag{34}$$

It should be mentioned that a few Gauss-Newton iterations based on the cost function in (15) could be applied to further refine the obtained source position estimates. A summary of the proposed method is given in Algorithm 1.

Algorithm 1 Summary of the proposed method.

Given received $\boldsymbol{r}$, the possible searching range of TDOA and FDOA τ_{max} and f_{max}, the initial source position set $\Xi = \{\hat{\boldsymbol{u}}_1^{(0)}, \cdots, \hat{\boldsymbol{u}}_{N_p}^{(0)}\}$, the tolerance ϵ and the maximum iteration times M
Generating the CAF surface of received signal pair $\boldsymbol{r}_k, k = 2, \cdots, K$ and $\boldsymbol{r}_1$ within the possible TDOA and FDOA range $\tau_{k,1} \in [-\tau_{max}, \tau_{max}]$ and $f_{k,1} \in [-f_{max}, f_{max}]$ using [32]
for $p = 1 : N_p$ **do**
  $\hat{\boldsymbol{u}}^{(0)} = \hat{\boldsymbol{u}}_p^{(0)}, m = 0$
  while $m < M$ **do**
    Step 1: Updating TDOA and FDOA estimates:
    Obtaining $\tilde{\boldsymbol{\theta}}_{k,1} = [\tilde{\tau}_{k,1}, \tilde{f}_{k,1}]^T$ by substituting $\hat{\boldsymbol{u}}^{(m)}$ into (6), and the covariance $\tilde{\boldsymbol{\Lambda}}_{k,1}$ by substituting $\boldsymbol{\Sigma}^{(m)}$ and $\hat{\boldsymbol{u}}^{(m)}$ into (25)
    Obtaining $\bar{\boldsymbol{\theta}}_{k,1} = [\bar{\tau}_{k,1}, \bar{f}_{k,1}]^T$ by finding the peak on the CAF surface within the confidence region in (26), and the covariance $\bar{\boldsymbol{\Lambda}}_{k,1}$ using the CRLB formulation
    Combining the TDOAs and FDOAs and their covariance matrices using (27) and (28)
    Step 2:Updating source position.
    Obtaining $\hat{\boldsymbol{u}}^{(m+1)}$ using $\boldsymbol{\theta}^{(m+1)}$ and $\boldsymbol{\Lambda}^{(m+1)}$ via the closed-form algorithms in [5,6,9,31] and $\boldsymbol{\Sigma}^{(m+1)}$ by substituting $\hat{\boldsymbol{u}}^{(m+1)}$ into (32)
    if $\|\hat{\boldsymbol{u}}^{(m+1)} - \hat{\boldsymbol{u}}^{(m)}\| < \epsilon$ **then**
      break
    end if
    $m = m + 1$
  end while
  $\hat{\boldsymbol{u}}_p = \hat{\boldsymbol{u}}^{(m+1)}$
end for
Selecting $\hat{\boldsymbol{u}}$ from $\hat{\boldsymbol{u}}_p, p = 1, 2, \cdots, N_p$ using (34)

4.2.2. Determination of D_x and D_y

We would like to obtain upper bounds for D_x and D_y such that they are chosen as large as possible to reduce computational complexity while keeping the local convergence rate very small. However, as far as we are concerned, there exist no such explicit criteria for the bounds. In [33], the monotonic convergence region $\Re_+$ of the EM-type method was defined as the largest open ball in parameter space with center $\boldsymbol{u}^0$ such that for each $\bar{\boldsymbol{u}}$ in $\Re_+$, we have

$$\begin{aligned} &\boldsymbol{A}_1 \succ \boldsymbol{O} \\ &\|\boldsymbol{A}_1^{-1}\boldsymbol{A}_2\| < 1, \forall \boldsymbol{u}, \end{aligned} \tag{35}$$

where $\boldsymbol{A}_1 = -\int_0^1 (1-\lambda)\nabla^{20}T\Big(\lambda\boldsymbol{u} + (1-\lambda)\boldsymbol{u}^0|\lambda\bar{\boldsymbol{u}} + (1-\lambda)\boldsymbol{u}^0\Big)d\lambda$, $\boldsymbol{A}_2 = \int_0^1 (1-\lambda)\nabla^{11}T\Big(\lambda\boldsymbol{u} + (1-\lambda)\boldsymbol{u}^0|\lambda\bar{\boldsymbol{u}} + (1-\lambda)\boldsymbol{u}^0\Big)d\lambda$ with $\nabla^{20}T(\boldsymbol{u}|\bar{\boldsymbol{u}}) = \frac{T(\boldsymbol{u}|\bar{\boldsymbol{u}})}{\partial\boldsymbol{u}\partial\boldsymbol{u}^T}$ and $\nabla^{11}T(\boldsymbol{u}|\bar{\boldsymbol{u}}) = \frac{T(\boldsymbol{u}|\bar{\boldsymbol{u}})}{\partial\boldsymbol{u}\partial\bar{\boldsymbol{u}}^T}$. $\boldsymbol{A} \succ \boldsymbol{O}$ means that $\boldsymbol{A}$ is positive definite. Using (35), one can increase the radius of $\Re_+$ gradually and determine the largest radius of $\Re_+$ which satisfies (35). Then D_x and D_y can be chosen according to the radius of $\Re_+$. However, it is rather tedious for us to evaluate (35) with the given radius, which usually involves a large number of Monte Carlo experiments. Note that the mainlobe of the cost function for positioning becomes narrower as the signal observation interval and signal bandwidth increase. Smaller D_x and D_y should be selected for longer observation interval and larger signal bandwidth. In practice, one can also plot the surface of the cost function in (15) and determine D_x and D_y such that at least one point is selected within the mainlobe of the cost function. Theoretical bounds for D_x and D_y with analytic expressions are left for future research. Next the computational complexity of the proposed method is analyzed and compared with that of the conventional two-step methods and DPD methods.

4.2.3. Computational complexity analysis

Denote by N_f the number of FDOA candidates, and N_i the iteration number of the proposed method.

First we give the computational complexity of generating CAF surfaces, which are used both in two-step methods and the proposed method. For the calculation of CAF surface between observer k and reference observer, a computational complexity of approximately $\mathcal{O}(N\log_2(N))$ is required for each FDOA candidate f. Therefore, the CAF surface is calculated with a complexity of $\mathcal{O}(N_f(K-1)N\log_2(N))$.

In our proposed method, during each iteration m for each initial source position $\hat{\boldsymbol{u}}_p^{(0)}$, TDOA and FDOA prediction and estimation values are calculated and Gaussian weighted fusion is required to obtain updated TDOA and FDOA, with a computational complexity of $\mathcal{O}(K^3)$. For the source position update in the second step, the computational cost mainly involves the multiplication, the inversion and singular value decomposition (SVD) of matrices of dimension $2(K-1)$, with a complexity of $\mathcal{O}(K^3)$. Thus the total computational complexity of the proposed method is $\mathcal{O}(N_f(K-1)N\log_2(N) + (K-1)N_iN_pK^3)$.

For the two-step methods, the TDOA/FDOA estimation complexity is given by $\mathcal{O}(N_f(K-1)N\log_2(N))$. And the second step is carried out with a computational complexity of $\mathcal{O}(K^3)$. Therefore, the complexity of two-step methods is $\mathcal{O}(N_f(K-1)N\log_2(N) + K^3)$. As multiple iterations and multiple initial source positions are required in our proposed method, it is computationally more demanding than the two-step methods, especially when the signal length N is relatively small. We also note here that the complexity of the proposed method increases as N_p increases.

For the grid search DPD methods, assume that the grid is established within a $2\Delta_x \times 2\Delta_y$ square around $\boldsymbol{u}^0$ with the search intervals being δ_x and δ_y in X and Y directions. For each grid point, a complexity of $\mathcal{O}((K-1)N\log_2(N))$ is required, which accounts for the total computational complexity of DPD methods being $\mathcal{O}(4\lceil\frac{\Delta_x}{\delta_x}\rceil\lceil\frac{\Delta_y}{\delta_y}\rceil(K-1)N\log_2(N))$. As $N_f \ll 4\lceil\frac{\Delta_x}{\delta_x}\rceil\lceil\frac{\Delta_y}{\delta_y}\rceil$, the complexity of the proposed method is much smaller than that of the DPD methods.

When the observers are stationary, the FDOA information is ignored and one can simply set $N_f = 1$ in above analyses.

5. Simulation results

In this section, simulations are conducted to reveal the localization performance and computational complexity of the proposed method. The source position is given by $\boldsymbol{u}^0 = [10, -10]^T$ m, and we assume that the *a priori* localization region is a 2000 m × 2000 m square centered at $\boldsymbol{u}^0$. A total of $K = 5$ observers are introduced for source localization, with their positions being the same as that in [17]. The observers' coordinates are $\boldsymbol{p}_1 = [-1000, -1000]^T$ m, $\boldsymbol{p}_2 = [-1000, 1000]^T$ m, $\boldsymbol{p}_3 = [0, 1000]^T$ m, $\boldsymbol{p}_4 = [1000, -1000]^T$ m, $\boldsymbol{p}_5 = [1000, 1000]^T$ m, respectively. Their velocities are $\boldsymbol{v}_1 = [5, -5]^T$ m/s, $\boldsymbol{v}_2 = [0, -10]^T$ m/s, $\boldsymbol{v}_3 = [-5, 5]^T$ m/s, $\boldsymbol{v}_4 = [10, 0]^T$ m/s, $\boldsymbol{v}_5 = [5, 0]^T$ m/s. The source signal is a Gaussian-shaped chirp signal [24] with $B = 0.3$ MHz, and its baseband form is given by

$$x(t) = \exp\{-\gamma t^2 + j2\pi K_w t^2\}, \tag{36}$$

where $K_w = \frac{B}{T}$ and T is the signal observation interval. γ is the attenuating factor, and we set $\gamma = 500$ in the whole simulation. The sampling frequency is $f_s = 5$ MHz. The SNR of signal is defined as the SNR of the reference observer, i.e., SNR_1. The relative amplitude at other observers are given as $a_{2,1} = 0.8$, $a_{3,1} = 1.1$, $a_{4,1} = 1$, $a_{5,1} = 0.9$. For our proposed method, we set $D_x = D_y = 100$ m empirically and $\epsilon = 10^{-3}$.

As comparisons, the localization results of several other methods are also shown. The first one is the two-step approach, where the TDOA/FDOA estimates are obtained using the methods in [34] (TDOA only) and [32] (TDOA/FDOA) during the first step. For source position determination, the iterative constrained weighted least squares (ICWLS) method in [31] is resorted to. The reason for selecting the above works as the two steps for the two-step method is that they are proved to be accurate when SNR is high. If the SNR is low and the localization estimates of two-step methods are out of the *a priori* region (outliers), these unbounded estimates are replaced with points randomly selected within this region. The second one is the grid search DPD method given in [16] (TDOA only) or [18] (TDOA/FDOA), and the cost function is given in (16). The grid search interval is set to be $\delta_x = \delta_y = 5$ with $\Delta_x = \Delta_y = 1000$ so as to find a coarse estimate, which is followed by refined grid search in the vicinity of this coarse estimate. The third one is the GN based DPD method [29], where the first and second order partial derivatives of (15) w.r.t. unknown parameters are constructed to yield the steepest descent directions. The initial solutions of GN based DPD are chosen as the localization results of two-step method. Furthermore, the corresponding CRLB curve for DPD is plotted. All the results are obtained from a total of 500 independent Monte Carlo runs.

5.1. TDOA only source localization

In this subsection, the simulation results in TDOA-only source localization scenario are provided. All the observers are stationary, i.e., $\boldsymbol{v}_k = \boldsymbol{0}$. Under this circumstance, we simply set $\phi_{k,1} = 0$ thus $b_{k,1} = a_{k,1}$.

First, the effect of SNR on localization performance is discussed. In Fig. 1, the localization RMSEs of different methods are shown in terms of varying SNRs, where $T = 2$ ms. As depicted in Fig. 1, when SNR_1 is relatively low, the two-step method yields poor localization precision, with its localization RMSE in log scale being higher than the proposed method by approximately 8 dB. The localization RMSE of the proposed method in log scale drops from 16dB to less than 4 dB as SNR_1 increases from −15 dB to 0 dB, although it is about 5 dB higher than that of the grid search DPD method. The reason that our proposed method is inferior to the

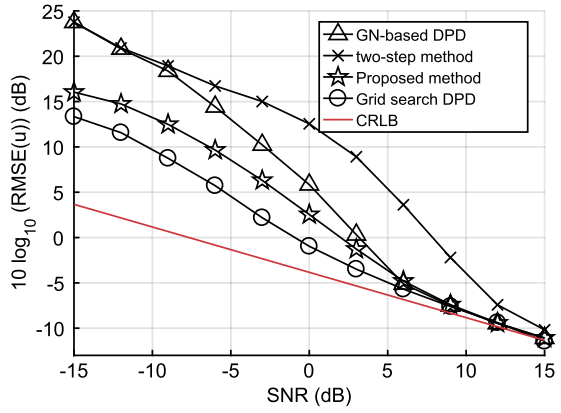

Fig. 1. Localization RMSEs of different methods with regard to varying SNR's. $B = 0.3$ MHz, $f_s = 5$ MHz, $N = 10,000$.

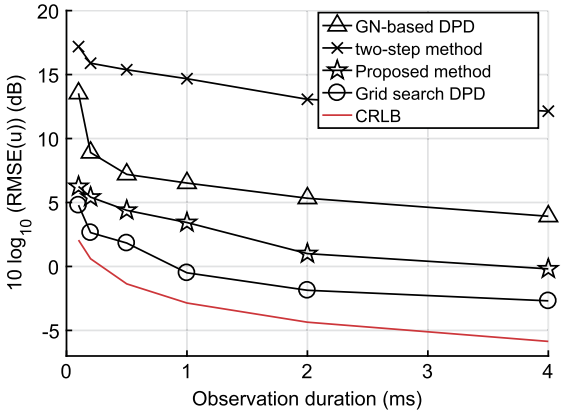

Fig. 2. Localization RMSEs of different methods under different signal observation durations. $B = 0.3$ MHz, $f_s = 5$ MHz, SNR $= 0$ dB.

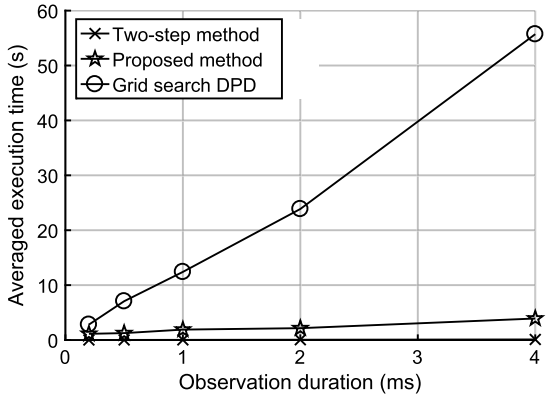

Fig. 3. Averaged execution times of different methods for TDOA-only localization (in seconds). $B = 0.3$ MHz, $f_s = 5$ MHz, SNR $= 0$ dB.

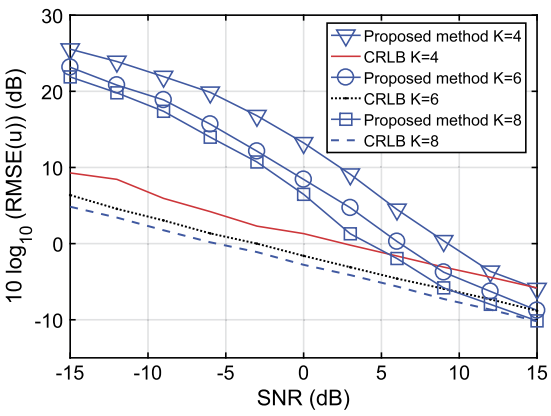

Fig. 4. Localization RMSEs of different methods under varying observer numbers with random observer locations. $B = 0.3$ MHz, $f_s = 5$ MHz, $N = 5,000$.

grid search DPD is that in our method TDOA and FDOA are estimated and thus information loss is introduced. Moreover, the GN based DPD method is also inferior to the proposed method due to its higher local convergence rate. As SNR_1 increases, these methods tend to approach the CRLB curve gradually. It is worth mentioning that the grid search DPD method could not reach the CRLB until the SNR exceeds 10 dB. This is caused by the fact that the cost function in (16) is highly non-convex with a considerable number of local optima. When the SNR is not high enough, the highest peak on cost function surface does not fall within the small error region due to the perturbation caused by random noises. As our proposed method focuses on reducing the computational load of the grid search DPD rather than suppressing the local optima, it is also subject to local convergence. Further studies on mitigating the local convergence are left for future researches.

To reveal the effect of signal observation duration T on localization performance, we set $\text{SNR}_1 = 0$ dB and increase T gradually. In Fig. 2, RMSEs of different methods are plotted as a function of T. One could find that the localization RMSEs of all these methods decrease consistently as T increases. The reason behind this phenomenon is that longer accumulation time of received source signal could improve the TDOA estimation accuracy and thus reduce the localization error. The proposed method works better than the two-step method and the GN based DPD method although it performs a little worse than the grid search DPD method. As SNR_1 is relatively low, the CRLB cannot be reached for the proposed method and the grid search DPD method, which is also due to the existence of local convergence as mentioned above.

In Fig. 3, the averaged execution times of different methods under varying observation durations are provided. The simulation setup is the same as that produces Fig. 2. As shown in Fig. 3, the two-step method requires the least execution time, and the grid search DPD method consumes much longer time than the proposed method, especially when the observation duration is long. This coincides with our theoretical computational complexity analysis results in Section 4. From the computational complexity perspective, the proposed method is more appealing compared to the grid search DPD, especially in localization applications where the computational resources are limited.

Next, the performance of the proposed method under varying observer numbers is provided. We set $T = 1$ ms, and the relative amplitudes are $a_{k,1} = 1, k = 2, 3, \cdots, K$. Without loss of generality, the observer numbers are selected to be $K = 4$, $K = 6$ and $K = 8$, respectively. As the optimal observer configuration is out of scope of this paper, the observer positions $\boldsymbol{p}_k, k = 1, 2, \cdots, K$ are deployed randomly within the *a priori* region to take into account the effects of observer position on localization RMSE. The RMSEs of the proposed method in log scale and the CRLBs are shown as a function of SNR for different observer numbers in Fig. 4.

The results in Fig. 4 indicate that the localization accuracy improves as the SNR or observer number increases, which coincides with our intuition. The SNR value required to approach the CRLB does not decrease with increased K for the proposed method. This is mainly due to the fact that the proposed method does not combine the information from all observers coherently, as is done in grid search DPD. Furthermore, as K increases, the improvement in localization accuracy caused by the increase of K becomes negligible, which is largely accounted for by the fact that the RMSE of the proposed method is inversely proportional to K.

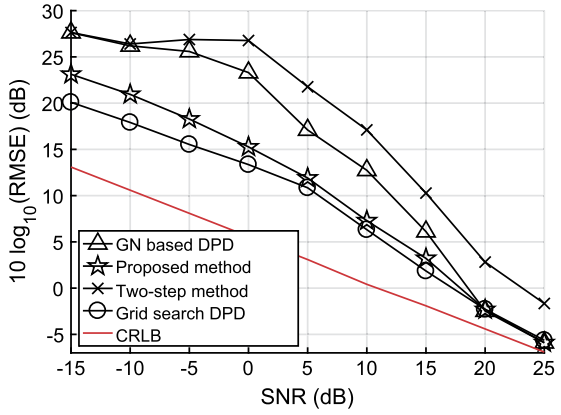

Fig. 5. Localization RMSEs of different methods with regard to varying SNRs. $B = 0.3$ MHz, $f_s = 5$ MHz, $N = 10,000$.

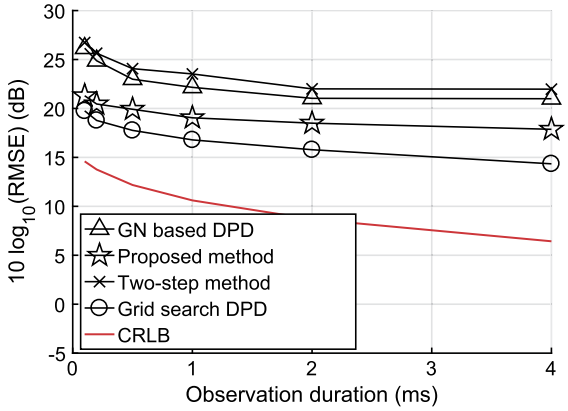

Fig. 6. Localization RMSEs of different methods under different signal observation durations. $B = 0.3$ MHz, $f_s = 5$ MHz, SNR $= -5$ dB.

5.2. Joint TDOA/FDOA localization

In this subsection, the FDOA information is combined with TDOA to jointly localize the source. The carrier frequency is $f_0 = 1$ GHz, and the phase shift is given by $\phi_{k,1} = (k-1)\pi/6$. The covariance matrix of TDOA and FDOA is determined using the CRLB expression in [24].

Fig. 5 depicts the RMSEs of different methods under varying SNRs. The signal observation interval is set to be $T = 2$ ms. From Fig. 5, one can observe that the proposed method has better localization accuracy under low SNRs ($\text{SNR}_1 < 0$ dB) compared to the two-step method and the GN based DPD method, although its RMSE in log scale is higher than the grid search DPD by about 3 dB. When SNR_1 is below 0 dB, the two-step method yields unbounded position estimates that are outside the region of interest and these results are manually reset randomly within the *a priori* region. As a result, its RMSE keeps perturbing around a constant value for $\text{SNR}_1 < 0$ dB. As SNR_1 increases, these methods approach the CRLB gradually. It is worth mentioning that the grid search DPD and the proposed method both could not reach the CRLB when SNR is not high, which is caused by the fact that the DPD cost function has a lot of local optima and the presence of noise may render the localization result deviate from the small localization error region. One may find that the localization CRLB given in Fig. 1 is lower than that in Fig. 5, which is counter-intuitive. The explanation for this phenomenon is that $\phi_{k,1} = 0$ is assumed known in Fig. 1 in the absence of frequency down conversion, such that source position is not coupled with the phase shift under this circumstance.

We then set $\text{SNR}_1 = -5$ dB, and evaluate the localization performance of these methods under varying signal observation intervals. Other settings remain the same as that produces Fig. 5. The results are shown in Fig. 6. As revealed in Fig. 6, the localization RMSEs of different methods decrease consistently as the observation duration increases. This is very intuitive because longer signal observation interval improves the TDOA and FDOA estimation accuracy and thus reduces the localization RMSE. The proposed method exhibits superior localization performance compared to the two-step method and the GN based DPD method, which could be explained by the introduction of the constraint during each iteration. Its RMSE is approximately 3 dB higher than the grid search DPD method because it is only an approximation to the latter. Note that even the grid search DPD method fails to approach the CRLB in this case because SNR_1 is relatively low such that the global optimum on cost function surface is not in small error region.

In Fig. 7, the averaged execution times of different methods are given under varying observation durations. The simulation setting is identical with the one that produces Fig. 6. From the figure, one

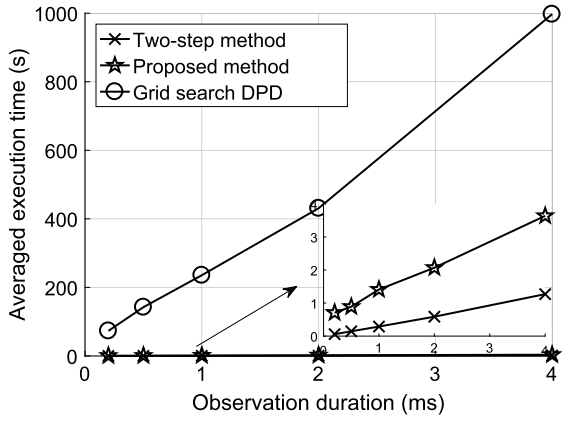

Fig. 7. Averaged execution times of different methods for joint TDOA and FDOA localization (in seconds). $B = 0.3$ MHz, $f_s = 5$ MHz, SNR $= -5$ dB.

can find that the two-step method requires very little execution time. The execution times of the proposed method and the grid search DPD method increase considerably with increased T. However, the proposed method has an acceptable execution time while the grid search DPD method requires much longer time. Particularly, when T exceeds 1 ms, the grid search DPD method requires several minutes to solve for the source position. The proposed method on the contrary, could yield almost realtime results for most cases. Therefore, the proposed method appears to be more suitable for applications in practice compared to the grid search DPD method from the perspective of computational complexity.

Finally, the RMSE of the proposed method in log scale is evaluated under $K = 4$, $K = 6$ and $K = 8$, respectively and compared with the corresponding CRLBs to reveal the effects of observer number on localization performance. We set $T = 1$ ms and $a_{k,1} = 1$ with $\phi_{k,1} = (k-1)\pi/8$. The observer positions are randomly selected within the region of interest and their velocities are also randomly chosen with a maximum velocity of 15 m/s. The simulation results are shown in Fig. 8.

As shown in Fig. 8, the RMSE of the proposed method decreases consistently as the SNR or K increases, because more observers would bring more information about the source position. Similar to Fig. 4, the improvement in localization RMSE becomes negligible as K increases because localization RMSE is generally inversely proportional to K. Due to the existence of local convergence, the proposed method requires a relatively high SNR to reach the corresponding CRLB.

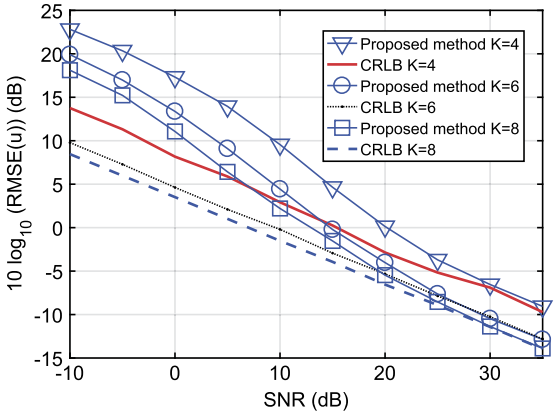

Fig. 8. Localization RMSEs of different methods versus varying observer numbers with random observer locations and velocities. $B = 0.3$ MHz, $f_s = 5$ MHz, $N = 10,000$.

6. Conclusion

In this paper, we focused on improving TDOA/FDOA localization performance with medium computational complexity, and a new EM-based localization method was proposed. During each iteration of the proposed method, the current source position estimate is used as a constraint to predict the TDOAs and FDOAs, which are combined with TDOA and FDOA estimates to yield renewed TDOA and FDOA measurements. The source position is updated using these renewed measurements in closed form. Simulation results showed that the proposed method outperformed the two-step method and the GN based DPD method in localization accuracy when the SNR is low, and it had much lower computational complexity compared to the grid search DPD method. Therefore, it is more appealing from the computational complexity perspective compared with the grid search DPD method. It should be noted that the rationale behind the proposed method could also be applied to other localization schemes.

Declaration of competing interest

The authors declare that they have no known competing financial interests or personal relationships that could have appeared to influence the work reported in this paper.

Acknowledgment

The authors would like to thank the anonymous reviewers for their valuable comments that have helped improve the quality of this paper.

References

[1] D.J. Torrieri, Statistical theory of passive location systems, IEEE Trans. Aerosp. Electron. Syst. AES-20 (2) (1984) 183–198, https://doi.org/10.1109/TAES.1984.310439.

[2] S. Tomic, M. Beko, R. Dinis, RSS-based localization in wireless sensor networks using convex relaxation: noncooperative and cooperative schemes, IEEE Trans. Veh. Technol. 64 (5) (2015) 2037–2050, https://doi.org/10.1109/TVT.2014.2334397.

[3] I. Guvenc, C.C. Chong, A survey on TOA based wireless localization and NLOS mitigation techniques, IEEE Commun. Surv. Tutor. 11 (3) (2009) 107–124, https://doi.org/10.1109/SURV.2009.090308.

[4] Y. Liu, F. Guo, L. Yang, W. Jiang, An improved algebraic solution for TDOA localization with sensor position errors, IEEE Commun. Lett. 19 (12) (2015) 2218–2221, https://doi.org/10.1109/LCOMM.2015.2486769.

[5] K.C. Ho, W. Xu, An accurate algebraic solution for moving source location using TDOA and FDOA measurements, IEEE Trans. Signal Process. 52 (9) (2004) 2453–2463.

[6] M. Sun, K.C. Ho, An asymptotically efficient estimator for TDOA and FDOA positioning of multiple disjoint sources in the presence of sensor location uncertainties, IEEE Trans. Signal Process. 59 (7) (2011) 3434–3440, https://doi.org/10.1109/TSP.2011.2131135.

[7] R. Amiri, F. Behnia, A. Noroozi, An efficient estimator for TDOA-based source localization with minimum number of sensors, IEEE Commun. Lett. 22 (12) (2018) 2499–2502, https://doi.org/10.1109/LCOMM.2018.2876525.

[8] J. Liang, Y. Chen, H. So, Y. Jing, Circular/hyperbolic/elliptic localization via Euclidean norm elimination, Signal Process. 148 (2018) 102–113, https://doi.org/10.1016/j.sigpro.2018.02.006.

[9] A. Noroozi, A.H. Oveis, S.M. Hosseini, M.A. Sebt, Improved algebraic solution for source localization from TDOA and FDOA measurements, IEEE Wirel. Commun. Lett. 7 (3) (2018) 352–355, https://doi.org/10.1109/LWC.2017.2777995.

[10] G. Wang, S. Cai, Y. Li, N. Ansari, A bias-reduced nonlinear WLS method for TDOA/FDOA-based source localization, IEEE Trans. Veh. Technol. 65 (10) (2016) 8603–8615, https://doi.org/10.1109/TVT.2015.2508501.

[11] Y. Wang, Y. Wu, An efficient semidefinite relaxation algorithm for moving source localization using TDOA and FDOA measurements, IEEE Commun. Lett. 21 (1) (2017) 80–83, https://doi.org/10.1109/LCOMM.2016.2614936.

[12] A. Amar, A.J. Weiss, Direct position determination in the presence of model errors–known waveforms, Digit. Signal Process. 16 (1) (2006) 52–83, https://doi.org/10.1016/j.dsp.2005.03.003.

[13] A.J. Weiss, A. Amar, Direct geolocation of stationary wideband radio signal based on time delays and Doppler shifts, in: 2009 IEEE/SP 15th Workshop on Statistical Signal Processing, 2009, pp. 101–104.

[14] A. Amar, A.J. Weiss, Direct position determination (DPD) of multiple known and unknown radio-frequency signals, in: 2004 12th European Signal Processing Conference, 2004, pp. 1115–1118.

[15] A.J. Weiss, Direct geolocation of wideband emitters based on delay and Doppler, IEEE Trans. Signal Process. 59 (6) (2011) 2513–2521, https://doi.org/10.1109/TSP.2011.2128311.

[16] N. Vankayalapati, S. Kay, Q. Ding, TDOA based direct positioning maximum likelihood estimator and the Cramer-Rao bound, IEEE Trans. Aerosp. Electron. Syst. 50 (3) (2014) 1616–1635, https://doi.org/10.1109/TAES.2013.110499.

[17] E. Tzoreff, A.J. Weiss, Expectation-maximization algorithm for direct position determination, Signal Process. 133 (2017) 32–39, https://doi.org/10.1016/j.sigpro.2016.10.015.

[18] J. Li, L. Yang, F. Guo, W. Jiang, Coherent summation of multiple short-time signals for direct positioning of a wideband source based on delay and doppler, Digit. Signal Process. 48 (2016) 58–70, https://doi.org/10.1016/j.dsp.2015.09.008.

[19] L. Tzafri, A.J. Weiss, High-resolution direct position determination using MVDR, IEEE Trans. Wirel. Commun. 15 (9) (2016) 6449–6461, https://doi.org/10.1109/TWC.2016.2585116.

[20] M. Pourhomayoun, M.L. Fowler, Distributed computation for direct position determination emitter location, IEEE Trans. Aerosp. Electron. Syst. 50 (4) (2014) 2878–2889, https://doi.org/10.1109/TAES.2014.130005.

[21] J. Bosse, A. Ferreol, P. Larzabal, Performance analysis of passive localization strategies: direct one step approach versus 2 steps approach, in: 2011 IEEE Statistical Signal Processing Workshop (SSP), 2011, pp. 701–704.

[22] L. Yang, K.C. Ho, An approximately efficient TDOA localization algorithm in closed-form for locating multiple disjoint sources with erroneous sensor positions, IEEE Trans. Signal Process. 57 (12) (2009) 4598–4615, https://doi.org/10.1109/TSP.2009.2027765.

[23] S. He, X. Dong, High-accuracy localization platform using asynchronous time difference of arrival technology, IEEE Trans. Instrum. Meas. 66 (7) (2017) 1728–1742, https://doi.org/10.1109/TIM.2017.2666278.

[24] A. Yeredor, E. Angel, Joint TDOA and FDOA estimation: a conditional bound and its use for optimally weighted localization, IEEE Trans. Signal Process. 59 (4) (2011) 1612–1623, https://doi.org/10.1109/TSP.2010.2103069.

[25] S. Stein, Algorithms for ambiguity function processing, IEEE Trans. Acoust. Speech Signal Process. ASSP-29 (3) (1981) 588–599.

[26] X. Xiao, F. Guo, D. Feng, Low-complexity methods for joint delay and Doppler estimation of unknown wideband signals, IET Radar Sonar Navig. 12 (4) (2018) 398–406, https://doi.org/10.1049/iet-rsn.2017.0368.

[27] T.K. Moon, The expectation-maximization algorithm, IEEE Signal Process. Mag. 13 (6) (1996) 47–60, https://doi.org/10.1109/79.543975.

[28] D. Musicki, R. Kaune, W. Koch, Mobile emitter geolocation and tracking using TDOA and FDOA measurements, IEEE Trans. Signal Process. 58 (3) (2010) 1863–1874, https://doi.org/10.1109/TSP.2009.2037075.

[29] S.M. Kay, Fundamentals of Statistical Signal Processing: Estimation Theory, PTR Prentice Hall, 1993.

[30] A. Azevedo-Filho, R.D. Shachter, Laplace's method approximations for probabilistic inference in belief networks with continuous variables, in: Uncertainty Proceedings 1994, Morgan Kaufmann, 1994, pp. 28–36.

[31] X. Qu, L. Xie, W. Tan, Iterative constrained weighted least squares source localization using TDOA and FDOA measurements, IEEE Trans. Signal Process. 65 (15) (2017) 3990–4003, https://doi.org/10.1109/TSP.2017.2703667.

[32] R. Tao, W.Q. Zhang, E.Q. Chen, Two-stage method for joint time delay and Doppler shift estimation, IET Radar Sonar Navig. 2 (1) (2008) 71–77, https://doi.org/10.1049/iet-rsn:20060014.

[33] A.O. Hero, J.A. Fessler, Asymptotic Convergence Properties of EM-Type Algorithms, EECS Univ. of Michigan, Ann Arbor, MI, 1993, pp. 1–31.
[34] C. Knapp, G. Carter, The generalized correlation method for estimation of time delay, IEEE Trans. Acoust. Speech Signal Process. ASSP-24 (4) (1976) 320–327.

Fuhe Ma is now a Ph.D. candidate in National University of Defense Technology (NUDT), Changsha, Hunan China. He received his M.Sc. degree in statistical signal processing from NUDT in 2016. His research interests include passive localization and statistical signal processing.

Fucheng Guo received the B.S. and Ph.D. degrees from the National University of Defense Technology (NUDT), Changsha, Hunan China, in 1998 and 2002, respectively. From 2006 to 2007, he was a visiting scientist at the Xi'an Jiaotong University, Xi'an, Shanxi China. From 2009 to 2010, he was a visiting scholar at the University of Missouri, Columbia, MO USA. Currently, he is a professor with the NUDT. His current research interests include passive localization, tracking and radar signal processing.

Le Yang received the B.Eng. and M.Sc. degrees in Electrical Engineering from the University of Electronic Science and Technology of China (UESTC), Chengdu, China, in 2000 and 2003, respectively. He received the Ph.D. degree in Electrical and Computer Engineering in 2010 from the University of Missouri, Columbia, MO USA. Between 2003 and 2004, he was a lecturer at the UESTC. From 2004 and 2005, he was with the University of Victoria, Victoria, BC, Canada, working on diversity techniques and performance evaluation of communication systems. In January 2006, he transferred to the McMaster University, Hamilton, ON, Canada, where he focused his research on artificial neural networks and computational neuroscience. From 2011 to 2018, he was an associate Professor with the Jiangnan University, Wuxi, Jiangsu China. Since 2019, he has been with the Department of Electrical and Computer Engineering, University of Canterbury, Christchurch, 8020, New Zealand. His current research interests include sensor networks, passive localization, tracking and machine learning.